Energy influx from an rf plasma to a substrate during plasma processing

H. Kersten, E. Stoffels, W. W. Stoffels, M. Otte, C. Csambal, H. Deutsch, and R. Hippler

Citation: Journal of Applied Physics **87**, 3637 (2000); doi: 10.1063/1.372393
View online: http://dx.doi.org/10.1063/1.372393
View Table of Contents: http://scitation.aip.org/content/aip/journal/jap/87/8?ver=pdfcov
Published by the AIP Publishing

Energy influx from an rf plasma to a substrate during plasma processing

H. Kersten[a)]
Institute for Physics, University of Greifswald, Domstrasse 10a, D-17487 Greifswald, Germany

E. Stoffels and W. W. Stoffels
Department of Physics, TU Eindhoven, P.O. Box 513, 5600MB Eindhoven, The Netherlands

M. Otte, C. Csambal, H. Deutsch, and R. Hippler
Institue for Physics, University of Greifswald, Domstrasse 10a, D-17487 Greifswald, Germany

(Received 19 July 1999; accepted for publication 18 January 2000)

The energy influx delivered by an rf plasma to a metal substrate has been studied by a calorimetric method with a thermal probe. By changing the substrate voltage, the influence of the kinetic energy of the charge carriers to the thermal power could be determined. The measured energy influx for an argon plasma can be explained mainly by ions, electrons, and their recombination. In the case of an oxygen plasma, where the energy influx is under comparable conditions about 50% higher, also other transfer mechanisms such as surface-aided atom association and relaxation of rovibrational states have to be taken into consideration. © *2000 American Institute of Physics.* [S0021-8979(00)05608-5]

I. INTRODUCTION

Plasma wall interactions are of great importance in a large variety of applications of low-temperature, low-pressure plasmas such as in etching, deposition, and surface modification of thin films. In these complex processes, the thermal and energetic conditions at the substrate surface play a dominant role.

The thermal conditions at the substrate surface affect elementary processes like adsorption, desorption, and diffusion as well as chemical reactions (chemical sputtering, surface film reaction).[1–3] On the other hand, especially in the case of thin film deposition, the microstructure and morphology as well as the stoichiometry of the film depend strongly on the energetic conditions at the surface.[4,5] Also, surface diffusion of adsorbed atoms can be enhanced, which results in a rearrangement of deposited atoms.[6] In addition, bombardment of a growing film with low-energy ions results in a modification of film properties such as adhesion and residual stress, etc.[7]

It should be emphasized that in addition to external heating, the surface temperature T_S is largely influenced by the energy flux J_{in} resulting from energetic particle bombardment, chemical surface reactions and heat radiation.[8,9] By a suitable variation of the experimental conditions, the different contributions to the substrate heating can be separated and independently studied.

In the present article, we perform investigations on the energy influx (thermal power) to substrates in rather weak rf discharges. In this type of discharge, used for deposition of coatings, cleaning, and conditioning of surfaces, the heat load on the surface is often a critical parameter. Also the heat load of microdisperse powder particles, suspended in a discharge is a topic under current investigation.[10,11] In Sec. II, the various heat sources and sinks of a substrate in a discharge will be discussed. In Sec. III, the design of our thermal probe is discussed along with the plasma setup. Measurements of the relevant plasma parameters like the electron density and temperature are presented to allow for a good comparison of the measured and calculated heat fluxes, which is shown in the final section.

II. THEORY

When a solid comes into contact with a plasma, energy transfer takes place. The substrate is heated and, after a certain time, it may reach a thermal equilibrium. This steady state is determined by a balance of energy gain from the plasma processes and energy losses by conduction and radiation.[12,13] The general power balance at the substrate is given by

$$Q_{\text{in}} = \dot{H}_S + Q_{\text{out}}, \tag{1}$$

where $\dot{H}_S = mc(dT_S/dt)$ denotes the enthalpy of the substrate and Q_{out} summarizes the heat losses by radiation and thermal conduction by the gas and the substrate. For most substrates thermal conduction to (or from, in case of a heated substrate) the substrate holder will be the dominant heat sink (source). However, in case of an isolated substrate, like a trapped microdisperse particle floating in the discharge, this is completely absent. In those cases, radiation and gas cooling are the only heat sinks. As we operate at low pressures and low temperatures, both are relatively ineffective and thus the temperature of a thermally isolated object in a discharge can be elevated with respect to its surroundings.[10]

In the following, the different contributions to the total energy influx Q_{in} which are relevant under our experimental conditions will be discussed shortly. It should be mentioned that the flux Q_{in} is the surface integral of the related energy flux density J_{in} over the substrate surface A_S:

a)Electronic mail: kersten@physik.uni-greifswald.de

$$Q_{\text{in}} = \int_{A_s} J_{\text{in}} dA. \tag{2}$$

In general, the total energy influx J_{in} is the sum of the fluxes due to electrons (J_e), ions (J_i), neutrals (J_n), and photons (J_{phot}). Each of these fluxes consists of several contributions. The electrons and ions hitting a substrate transfer their kinetic energy, moreover recombination energy is released when a positive ion and electron recombine at the surface. In our case with cold gas and cold substrates, the kinetic energy of neutrals can be neglected, but neutrals can transfer internal energy from electronic and rovibrational excitation (J_{inter}). Furthermore gas molecules can associate with another gas phase species at the surface (J_{ass}) or react with the surface (J_{chem}). Heating by photons can occur by blackbody radiation from heated surfaces or by plasma produced photons. In our case, there are no heated surfaces and the metal substrate reflects virtually all photons in the visible region. At our operating pressure and power, the plasma is optically dense for resonant radiation and therefore the thermal load of UV photons hitting the substrate is also negligible. Note that this is not necessarily true in other plasma configurations or in case of opaque, nonreflecting substrates. Concluding, the total heat influx is given by

$$J_{\text{in}} = J_e + J_{\text{ion}} + J_{\text{inter}} + J_{\text{ass}} + J_{\text{chem}}. \tag{3}$$

In the following, we shall estimate these contributions in more detail. In general, the mean kinetic ion energy is determined by the ion energy distribution function (IEDF) at the surface. At elevated pressures, the energy distribution of the ions arriving at the substrate is affected by collisions in the sheath in front of the substrate. At low pressures in the present experiment (1 Pa), the maximum ion energy is determined mainly by the free fall energy $e_0 V_{\text{bias}}$, where V_{bias} is the potential drop from the plasma glow to the substrate which corresponds to the difference between the plasma potential V_{pl} and the substrate potential V_S with respect to ground:

$$V_{\text{bias}} = V_{\text{pl}} - V_S. \tag{4}$$

It should be emphasized that the simple expression of Eq. (4) for the mean kinetic energy of the ions striking the substrate is applicable in most cases of plasma processing. Only if the IEDF for the ions near the substrate is much more complex, the assumption of $e_0 V_{\text{bias}}$ for the kinetic energy is no longer justified. In an argon discharge, charge transfer reactions readily occur in the sheath region. In this case, part of the ion energy ($e_0 V_{\text{bias}}$) is transferred to a neutral. However, as the neutral has a directional velocity towards the substrate, still most energy will be transferred to the substrate and the simple expression of Eq. (4) holds. In addition to the directed kinetic energy of the ions, which originates from acceleration in the electrical field in front of the substrate, the ions also have thermal energy. However, this part can be neglected because the ions are nearly at room temperature. Hence, the contribution of the kinetic energy of the ions (J_i^{kin}) which can be expressed as a product of the ion flux density j_i and their mean energy E_i is given by

$$\begin{aligned} J_i^{\text{kin}} &= j_i E_i = j_i e_0 (V_{\text{pl}} - V_S) \\ &= n_e v_{\text{amb}} e_0 (V_{\text{pl}} - V_S) \\ &= n_e \sqrt{\frac{kT_e}{m_i}} \exp\{-0.5\} e_0 (V_{\text{pl}} - V_S), \end{aligned} \tag{5}$$

where we have approximated the ambipolar diffusion $n_e v_{\text{amb}}$ in Eq. (5) by the Bohm flux[14]

$$j_i = n_e \sqrt{\frac{kT_e}{m_i}} \exp\{-0.5\}. \tag{6}$$

Under low-pressure conditions ($p < 10$ Pa), the Bohm equation is applicable for argon discharges, because in the presheath almost no collisions occur. The Bohm equation yields the ion flux j_i by knowing the ion density n_i, which equals the electron density n_e at the sheath edge. This approach is also valid in presence of negative ions, like in an oxygen discharge. However, in that case the Bohm flux [Eq. (6)] is governed by the ion temperature.[15]

In addition to kinetic energy, ions transfer a part of their potential energy when striking a surface. For metallic substrates, the neutralization of ions is caused by long-range interactions and may be accompanied by the emission of secondary electrons. The resulting contribution J_i^{rec} to the energy balance of the substrate due to the recombination is

$$J_i^{\text{rec}} = j_i E_{\text{rec}}. \tag{7}$$

Each incident ion releases its ionization potential E_{ion} minus the work function of the metal Φ, as an electron has to be released from the metal surface before recombination. In case of secondary electron emission, also their work function has to be supplied. The released recombination energy E_{rec} is given by

$$E_{\text{rec}} = E_{\text{ion}} - \Phi. \tag{8}$$

Data for E_{ion} and Φ, respectively, may be taken from the literature.[16] In principle, Eq. (8) should still be corrected by the difference between the adsorption energy of the ion and the desorption energy of the resulting neutral, but this contribution is rather low. As stated above, it is assumed that the resulting neutral is in its ground state, especially for molecular ions, this is not necessarily true and appropriate changes in E_{ion} should be made in this case.

The cooling effect by sputtering of substrate material can also be ignored. Because in our case, the energy $e_0 V_{\text{bias}}$ of the impinging ions is always smaller than 100 eV, the sputter yield Y is rather small ($Y \leqslant 0.1$). Therefore, the flux of sputtered surface atoms, which may contribute to an energy loss of the substrate, is negligible.

The electrons have to overcome the bias voltage V_{bias} in front of the substrate in order to reach the substrate surface and to transfer their energy. The kinetic energy of the plasma electrons arises from the integration over the EEDF from V_{bias} up to infinity. Moreover, every electron hitting the surface will release an energy equivalent to the work function of the material. In case of a Maxwellian electron energy distribution (EEDF), the energetic influx J_e thus reads

$$J_e = n_e \sqrt{\frac{kT_e}{2\pi m_e}} \exp\left\{-\frac{e_0 V_{\text{bias}}}{kT_e}\right\} 2kT_e. \tag{9}$$

The energy, which the electrons lose by overcoming the bias potential, is stored as potential energy in the electric field and consumed by accelerating ions hitting the substrate and by secondary electrons accelerated towards the plasma. This effect is taken into account by the work function Φ in Eq. (8). Both summands of the electron energy ($2kT_e$, Φ) are of the same order of magnitude.

Using the general equations (4)–(9) listed above, an analysis of the charged plasma components will yield, in principle, the surface heating caused by positive ions and electrons. In case of electronegative plasmas like oxygen, negative ions also have to be considered. Because of their low temperature, they can only reach the substrate if there is a large positive bias. Therefore, in general, negative ions can be neglected in the thermal balance of a substrate. As the energy flux of the charged species strongly depends on the bias potential of the substrate [Eqs. (5) and (9)], it is possible to separate their contribution from other heat sources like radiation, chemical reactions, neutrals, and charge carriers, by variation of the bias potential.

The contribution of the various neutral gas components strongly depends on the gas composition and the plasma conditions. In a process plasma containing reactive species (N_2,O_2, etc.), surface-aided atomic association and heterogeneous exothermic reactions occur. Evidence for substrate heating by exothermic reactions on the processed surface has been reported, for example, in case of plasma etching of silicon with fluorine containing compounds[17] and during plasma cleaning of contaminated metal surfaces.[18] In the case of atomic recombination as a special surface reaction process, the fraction of the energy transferred to the solid has been described for example in Ref. 19. The percentage of the recombination energy, which is used for surface heating, varies with the chemical composition of the surface. Furthermore, relaxation of internal energy (electronic and rovibrational excitations) adds to the thermal influx to a substrate. Energy transfer of argon metastable atoms and rovibrationally excited molecular species to microdisperse particles floating in the discharge has been suggested by Stoffels and Stoffels.[20]

The energy influx by internal energy transfer J_{inter}, atom recombination J_{ass} and exothermic reactions J_{chem} is described by

$$J_{\text{ass}} = j_{\text{O}} \Gamma_{\text{O}} E_{\text{diss}} = \Gamma_{\text{O}} \frac{1}{2} n_{\text{O}} \sqrt{\frac{8kT_g}{\pi m_{\text{O}}}} E_{\text{diss}}, \tag{10}$$

in which Γ is the energy transfer, association, or reaction probability of the neutrals on the substrate surface and j its flux density. The latter can be determined accurately, if the species density and its diffusion properties are known.[21] The index O indicates the quantities for oxygen. At low pressures, a rough estimate is obtained by simply multiplying the global species density n with its thermal velocity v: $j = nv$.

If the chemical reactions result in layer formation, one can easily estimate J_{chem} from the growth rate R_{dep}, the mass density ρ of the layer, and the average specific enthalpy gain h_{ox}.

$$J_{\text{chem}} = R_{\text{dep}} \rho h_{\text{ox}}. \tag{11}$$

Analogous formulas can be easily derived in case of etching a substrate, in which the reaction products are volatile.

The thermal load on a substrate resulting from plasma photons can be calculated by integrating the product of photon flux $\Phi_{\text{pl}}(\nu)$, photon energy $h\nu$, and absorption coefficient of the surface $A(h\nu)$ over the complete spectral range.

$$J_{\text{phot}} = \int \Phi_{\text{pl}}(\nu) h\nu A(h\nu) d\nu. \tag{12}$$

The photon flux has to be estimated using a radiative plasma model.

The different energetic contributions calculated on the basis of the equations mentioned above can be compared with the total energy influx J_{in} measured by the probe method described below. This comparison gives insight into the processes involved and about the dominant mechanisms determining the thermal balance of a substrate during rf plasma treatment.

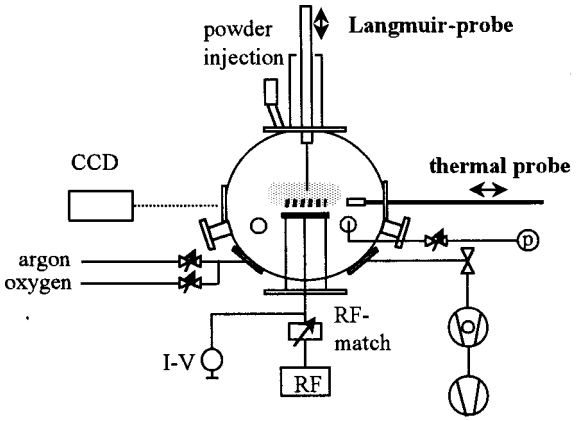

FIG. 1. Schematic of the experimental setup.

III. EXPERIMENT

A. Energy flux measurements by a thermal probe

The integral energy influx from the plasma towards the substrate can be measured by a simple thermal probe.[22] Previously, Thornton[23] and Wendt *et al.*[24] have proposed a similar procedure for the determination of the total heat influx. A schematic sketch of the setup is shown in Fig. 1. The probe is mounted on a manipulator arm to allow for horizontal and vertical scans. It can be also rotated, in order to measure directional fluxes, e.g., secondary electrons coming from an rf electrode or infrared photons from a heated surface.

In our experiments, the heat flux measurements are carried out by observing the rate of temperature rise dT_S/dt of a copper substrate (diameter: 3.4 cm, area $A_S = 18\,\text{cm}^2$, thickness: 0.02 cm) which is spot welded to a thermocouple (type *j*) and placed within a solid shield. The substrate is only connected to the thermocouple and a wire for additional biasing. No other contact to the shield and holder is realized

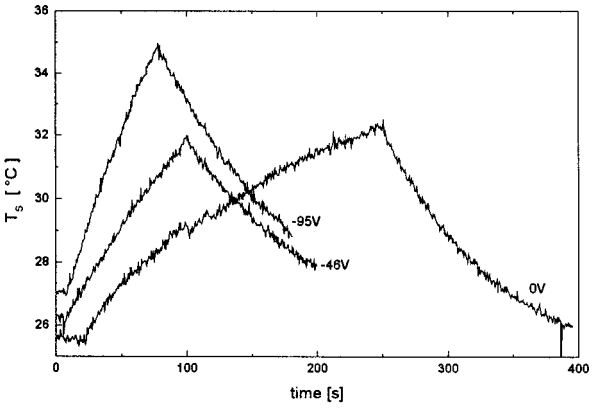

FIG. 2. $T_S(t)$ curves as measured during the Ar plasma process ($p=1$ Pa, $P=15$ W) for three substrate voltages (0, −46, −95 V).

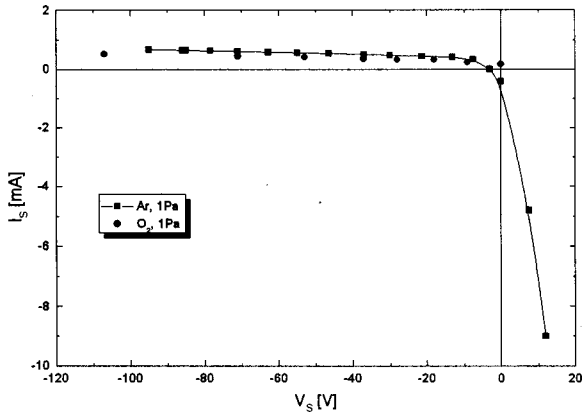

FIG. 3. Current–voltage characteristic of the substrate (thermal probe) for argon and oxygen.

in order to minimize thermal conduction. Because of its large heat capacity the shield is at a constant environmental temperature T_{env} during the time of the measurement.

The measurement of the total energy influx Q_{in} is based on the determination of the difference between the time derivatives of the substrate temperature T_s during heating (''plasma on'') and cooling (''plasma off''). Examples of typical temperature curves $T_S(t)$ which have been obtained for an Ar plasma ($p=1$ Pa, $P=15$ W) at three different substrate voltages are presented in Fig. 2.

The general power balance at the substrate is given by Eq. (1). The losses are always small in comparison to the incoming fluxes due to the plasma process. During the heating phase (plasma on: $Q_{\text{in}}>0$) $\dot{H}_S$ is determined by $\dot{H}_S(\text{heat})=Q_{\text{in}}-Q_{\text{out}}$ and during the cooling phase (plasma off: $Q_{\text{in}}=0$) by $\dot{H}_S(\text{cool})=-Q_{\text{out}}$. By taking these expressions into Eq. (1), the difference yields the energy influx:

$$Q_{\text{in}}=\dot{H}_S(\text{heat})-\dot{H}_S(\text{cool})=mc\left\{\left(\frac{dT_S}{dt}\right)_{\text{heat}}-\left(\frac{dT_S}{dt}\right)_{\text{cool}}\right\}_T. \tag{13}$$

If the slopes dT_S/dt are determined at the same temperature T and assuming no change of the environmental temperature T_{env}, which is achieved by short measurement times, the expression within the brackets of Eq. (13) is a quantity proportional to the thermal power at the substrate. In order to obtain absolute values of Q_{in}, the specific heat of the substrate (thermal probe) was determined by a known thermal power as described in Ref. 25 to $C_S=0.65$ J/K.

The measured energy influx is an integral value comprising the various contributions as kinetic energy of charge carriers, recombination heat, reaction heat, etc. By measuring the energy fluxes at different substrate voltages V_S, the contributions of ions and electrons from the other sources can be separated. For this purpose, the thermal probe (substrate) can be biased externally by a dc voltage. Simultaneously, the electrical current to the substrate is measured and one obtains the substrate characteristic, which is similar to a usual probe characteristic. In Fig. 3, the thermal probe characteristic in an 1 Pa argon and oxygen rf plasma is shown. At sufficiently negative substrate voltages, the current I_S changes only slightly with increasing voltage V_S. From the characteristics in Fig. 3, an ion saturation current of about 1 mA and a floating potential of $V_{\text{fl}}\approx -3$ V can be obtained for the argon plasma.

B. The plasma setup

In order to test the thermal probe, a commonly used asymmetric, capacitively coupled rf discharge was used. The plasma glow is located in the region between the plane aluminum rf electrode ($D=130$ mm) and the upper part of the spherically shaped reactor vessel ($D=400$ mm) which serves as grounded electrode, see Fig. 1.

The 13.56 MHz rf power is supplied by a generator (Dressler CESAR1310) in combination with an automatic matching network (Dressler VM700). The rf voltage was varied between 300 and 900 V, resulting in a discharge power of 10–100 W. The turbopump (Pfeiffer TMU260C) which allows for a base pressure of 10^{-4} Pa is connected to the vessel by a butterfly valve, the gas pressure was varied between 0.5 and 5 Pa by the valve and by using a flow controller (MKS). Argon and oxygen, respectively, were used as process gases.

C. Plasma diagnostics

In order to compare the measured energy fluxes with simple model assumptions, the internal plasma parameters of the rf discharge have been investigated by plasma diagnostics as analytical charge coupled device (CCD) photometry and Langmuir-probe measurements,[26] respectively.

A CCD camera (SBIG ST-6) coupled with a photoelectrical filter (CRI VIS2-05) was used to determine the sheath width in front of the powered electrode by measuring the spatial emission profile at several wavelengths. This gives information on the local variations in the electron energy distribution function, with a high spatial accuracy (0.2 mm).

The Langmuir-probe characteristics have been obtained by a source meter (Keithley SM2400). The probe (diameter: 47 μm, length: 12 mm) could be moved axially through the plasma bulk into the plasma glow near the sheath, see Fig. 1. During a measurement, the probe voltage is stepwise increased and the electrical probe current is recorded from the

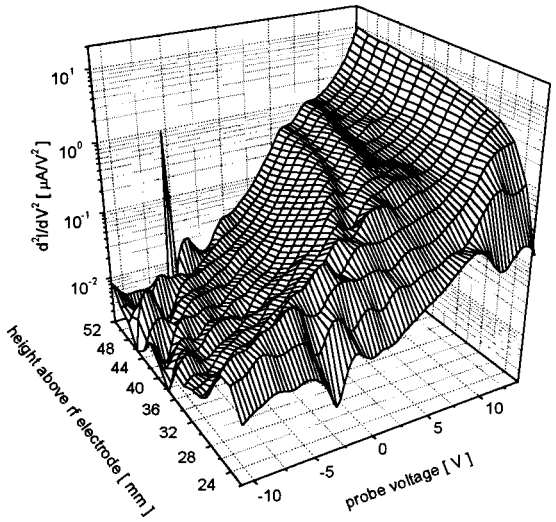

FIG. 4. Second derivative of Langmuir-probe characteristics, which is a measure for the EEDF obtained at different heights above the rf electrode ($p=0.75$ Pa, $P=10$ W).

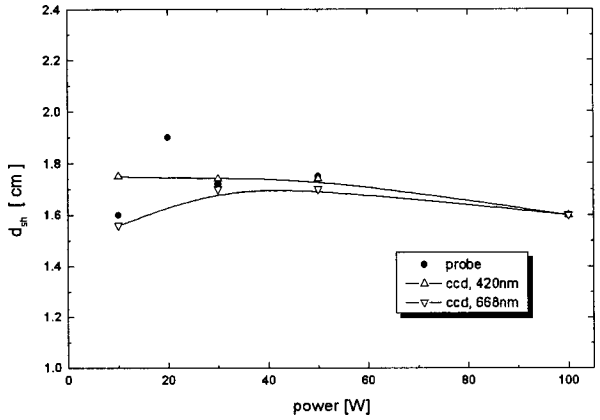

FIG. 5. Observed sheath thickness d_{sh} in front of the rf electrode for two wavelengths and determined by a Langmuir-probe for different rf power. The argon gas pressure was 1 Pa.

ion acceleration region up to the electron acceleration region. The electron energy distribution function (EEDF) can then directly be determined from the second derivative of the $V-I$ characteristics.[27] Figure 4 shows examples for the second derivative for argon at 0.75 Pa and 10 W taken at several distances above the electrode which yield Maxwellian distributions. The values of the electron density n_e and the mean electron energy $u_e(kT_e)$ as well as the plasma and floating potentials (V_{pl}, V_{fl}) have been determined from the probe's current–voltage characteristics.

IV. RESULTS AND DISCUSSION

A. Plasma parameters

The interpretation of the substrate heating by charge carriers requires the determination of the electron and ion density (n_e, n_i), the plasma and the floating potential (V_{pl}, V_{fl}), and the electron temperature (kT_e). In the present study, the internal plasma parameters have been measured in the substrate region by analytical CCD photometry and Langmuir-probe measurements as described above.

The sheath position has been determined by the CCD photometry technique. For example, the extension of the sheath thickness d_{sh} for an argon plasma has been estimated for two different excitation levels at 420 nm ($1s_5-3p_9$) and 668 nm ($1s_4-2p_1$). Figure 5 shows an example of the measured sheath width d_{sh} for $p=1$ Pa in dependence on the rf power. The accuracy of the determination of d_{sh} is ± 0.2 mm. Since the required energy for the excitation of the $2p$ level (13.48 eV) is lower than the excitation energy for the $3p$ level (14.5 eV), the glow in the 668 nm line can be observed closer to the electrode. This observation, which is known as Seeliger's rule of glow edge,[28] is due to the kinetic energy of γ electrons originating from the electrode and accelerated in the sheath. The larger the distance from the electrode, the more kinetic energy the electrons gain for exciting collisions.

In Fig. 5, the sheath widths measured by the CCD method are also compared with values obtained by Langmuir-probe measurements. In this case, d_{sh} was defined as the distance from the electrode where the $V-I$ characteristic of the Langmuir-probe failed. This means that within a distance of about 20 mm in front of the electrode (sheath), the second derivative of the probe characteristic, which is needed to determine the EEDF as well as the electron density and the electron temperature, is strongly disturbed and an evaluation of the probe characteristic becomes impossible. Both methods yield reliable values for the sheath thicknesses, but obviously the CCD method is more accurate. In systematic measurements, a weak dependence on the discharge power (Fig. 5), and a strong influence of the pressure on d_{sh} could be observed. In all cases the sheath thickness is in the order of a centimeter.

In addition, by using a balance equation,[29] the internal plasma parameters for an Ar plasma could also be obtained. Under the assumption that charge carrier formation occurs mainly by direct impact ionization within the plasma glow and by measuring the external discharge quantities as the amplitude of the rf voltage ($V_{pp} \sim V_{rf}$), the dc-bias voltage (V_{dc}) and the sheath thickness in front of the hot electrode, the model yields the electron temperature kT_e and electron density n_e.

The floating potential is $V_{fl}=-3$ V and the plasma potential V_{pl} is in the order of 15 V for argon and about 20 V for oxygen plasma, respectively. The plasma potential changes only slightly within the plasma glow. Figure 6 shows the variation of the plasma potential in an argon plasma as a function of the axial distance from the rf electrode. As mentioned above, the position where the potential drops dramatically and the evaluation of the EEDF fails can be identified as the sheath edge and it coincides with the optically determined sheath edge position (Fig. 5). A quite similar behavior can be observed in the axially measured electron temperature, shown in Fig. 7. At the sheath edge, there are hardly any electrons from the plasma glow. Most electrons are secondary electrons, heated in the sheath region. Thus, kT_e increases strongly towards the rf electrode, while the electron density n_e drops. The values at substrate position (3.25 cm), which are important for the calculations, are 3.5 eV for the argon plasma and about 5.2 eV for the

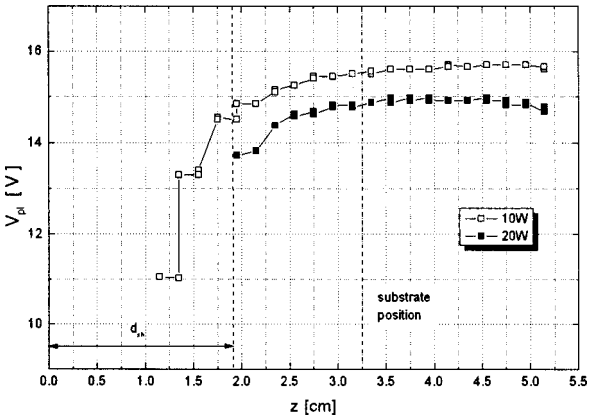

FIG. 6. Axially resolved plasma potential V_{pl} for an argon rf plasma at 1 Pa. The rf electrode is at $z=0$.

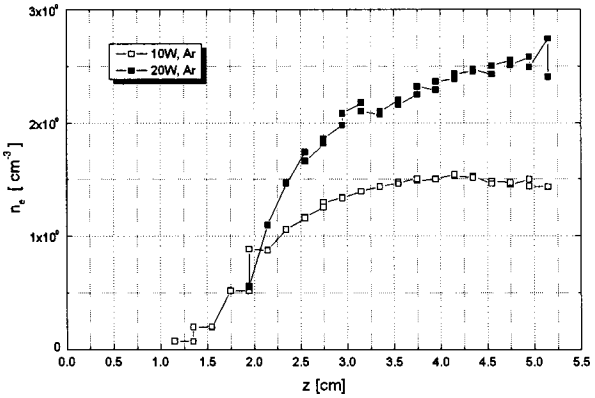

FIG. 8. Electron density n_e in dependence on axial position z.

oxygen plasma. For a Maxwellian EEDF, the electron temperature can also be simply estimated by the difference between floating and plasma potential:

$$V_{\mathrm{fl}}-V_{\mathrm{pl}}=\frac{kT_e}{2e_0}\ln\left(\frac{2.3m_e}{m_i}\right)\leqslant 0. \tag{14}$$

This formula yields for argon ($V_{\mathrm{fl}}-V_{\mathrm{pl}}=-18\,\mathrm{V}, m_e/m_i=1.4\times10^{-5}$), an electron temperature of 3.5 eV. By using the relevant values for oxygen, one obtains $kT_e=4.6\,\mathrm{eV}$. Comparison with the measurement supports the assumption of a Maxwellian EEDF at least for the argon plasma.

The electron density n_e for argon at a power of 15 W and a pressure of 1 Pa, which were the standard discharge conditions in energy flux measurements, is about $2\times10^9\,\mathrm{cm}^{-3}$ (Fig. 8). The values for the electron density and their dependence on discharge power determined by the Langmuir-probe measurements are also confirmed by the optical measurements on the basis of the sheath model.

B. Argon plasma

In the case of an argon plasma, we will initially consider the energetic contributions due to kinetic energy of the charge carriers [Eqs. (5) and (9)] and their recombination [Eq. (7)]. The contributions of the inert gas are limited, as there are no association and chemical reactions at the substrate surface. Only transfer of internal energy has to be considered.

In order to model J_e and J_i the internal plasma parameters obtained by Langmuir-probe measurements have been taken. The quantities are calculated for different substrate voltages V_S. The results are plotted in Fig. 9. It is obvious that for $V_S<V_{\mathrm{fl}}$, only the positive ions dominate the integral energy influx Q_{in}, while the contribution of electrons becomes important for $V_S>V_{\mathrm{fl}}$. In the range $V_S>0$, J_e increases dramatically due to the flux of electrons which is now drained by the substrate[25] acting as an additional disturbing electrode. Therefore, for positive substrate voltages, the model calculation on the basis of the Langmuir-probe measurements will fail and one should take the electron flux j_e which can be directly obtained from the substrate characteristic (Fig. 3):

$$j_e=\frac{I_S}{e_0A_S}. \tag{15}$$

The contribution by electrons for $V_S>0$ according to this expression is remarkably smaller than the values one obtains by assuming an undisturbed plasma and applying the

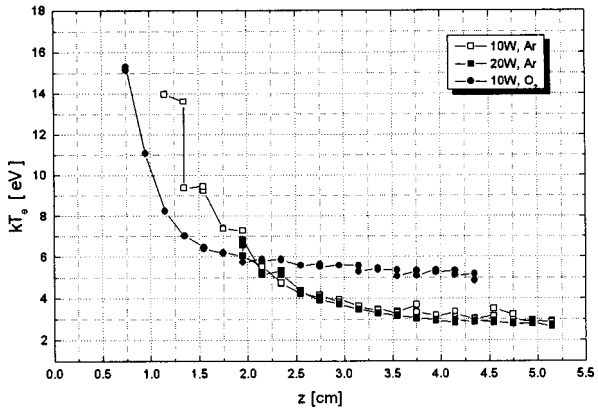

FIG. 7. Axially resolved electron temperature kT_e for argon and oxygen plasma, respectively, at 1 Pa. The sheath edge is at $z=1.9$ cm.

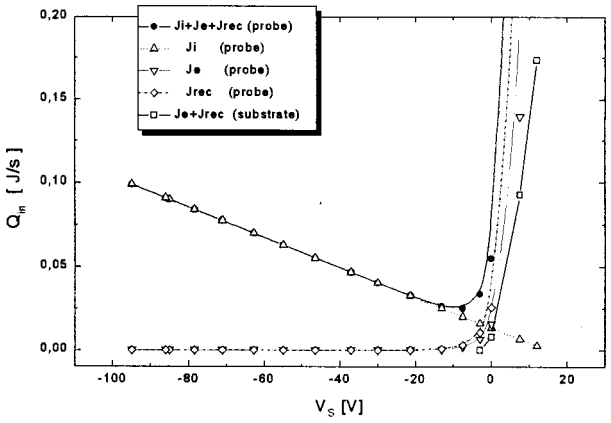

FIG. 9. Calculated contributions by ions (J_i,J_{rec}) and electrons (J_e) to the thermal balance of the substrate. The calculations are based on n_e measured by the Langmuir-probe and obtained by the substrate characteristics, respectively.

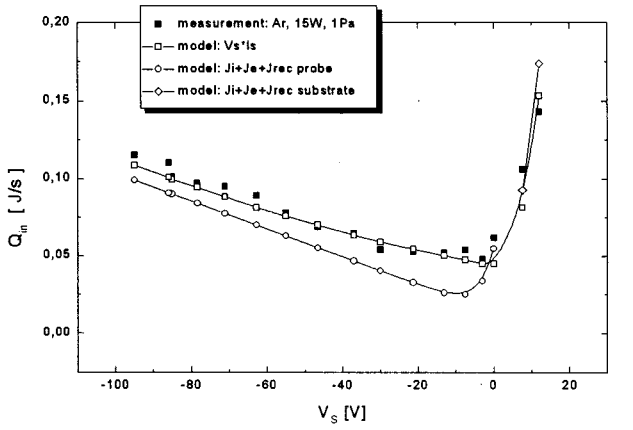

FIG. 10. Comparison of measured energy influx Q_{in} with several model assumptions for the different contributions.

Langmuir-probe measurements. This can be expected because a relatively large, positively biased thermal probe will significantly drain the electrons from the plasma. As a consequence, j_e and J_e are lowered.

The energy influx due to charged particles, if both electrons and ions are present, can also be estimated from the Bohm flux [Eq. (6)]. Assuming $j_e = j_i$ and remembering that in this case the electron energy flux can be neglected, the ion energy flux is simply given by $J_i = j_i(E_{\text{ion}} + eV_{\text{bias}})$. Substituting the electron density and temperature measured using the probe technique ($n_e = 2\times10^9\,\text{cm}^{-3}, kT_e = 3.5\,\text{eV}$) yields a total ion current to the thermal probe of 0.5 mA, which is in excellent agreement with the measured flux shown in Fig. 3. The total energy flux by ions for $V_s = V_{\text{fl}}$ to our probe thus is about 10^{-2} J/s, which remarkably agrees well with the extrapolated value for ion heating plotted in Fig. 9.

Finally, the measurements of the total energy influx as a function of the substrate voltage are shown in Fig. 10 for the different V_S regions. The influx Q_{in} measured by the thermal probe (solid squares) decreases with increasing substrate voltage in the range $V_S < V_{\text{fl}}$, reaches its minimum at $V_S = V_{\text{fl}}$ and increases again with the supplied voltage in the range $V_S > V_{\text{fl}}$. For sufficiently negative substrate voltages (left part of the graph), the ion saturation current j_i towards the substrate is nearly constant and the deposited thermal power depends only on the ion energy, which is given by the difference between the plasma and substrate potential. If this difference becomes smaller, the contribution J_i decreases. The model, which takes the Bohm criterion and the plasma parameter measured by the Langmuir-probe into account (open circles) reflects the experimentally obtained slope of J_{in} quite well. The constant difference between the two data sets reflects the heating by neutrals. The measurements at the right branch that means for positive substrate voltages have been modeled with the electron flux derived from the substrate characteristic shown in Fig. 3. In this region, the ions are not important, while the probe model yields electron contributions which are much too large.

It can be easily seen that the contribution of neutral species to the thermal load is about 2×10^{-2} J/s. In our case, the contribution of photons can be neglected. The plasma is optically dense for resonant photons, so they cannot reach the substrate, while photons in the optical region are reflected as the probe has a metallic surface. The energetic neutral species in an argon plasma are most likely the argon metastable states. Their density is about $10^{11}\,\text{cm}^{-3}$.[30] Indeed, following the estimation given in the theoretical part and assuming a total conversion at the surface, we find the missing thermal load.

Thus, in an argon plasma the integral energy influx J_{in} can be determined by a calorimetric method. It consists of the kinetic energy of charge carriers and their recombination energy and the energy released by relaxation of metastables. The contribution of ions (J_{ion}) and electrons (J_e) can be distinguished by a variation of the substrate potential V_S.

For practical purposes, a more simple description of the measured curve can be useful by taking

$$Q_{\text{in}} = Q_{\text{in}}(V_{\text{fl}}) + I_S V_S, \tag{16}$$

in which $Q_{\text{in}}(V_{\text{fl}})$ denotes the experimentally determined energy influx at floating potential. By this ''model'' (open squares in Fig. 10), one can clearly recognize that the whole electric power at the substrate is transferred into thermal power resulting in a certain thermal balance of the substrate. Especially for the ions, this excellent agreement means that the energy accomodation of Ar^+ ions at a metallic surface is close to unity. Recent investigations by Toyoda and Sugai[31] show that ion survival at the surface is less than 5%.

The results indicate that a description of the energy influx by charge carriers, which are characterized by plasma diagnostics (probe, substrate), is an appropriate method for the treatment of plasma-substrate interaction. Vice versa, by measuring the energy influx with a thermal probe and under the assumption of valid models for the different V_S regions, one can also get some information on the plasma data.

C. Oxygen plasma

The discussion of J_{in} in case of an oxygen plasma can be given, in principle, in a quite similar manner as it has been done for argon. In an oxygen discharge, there are three main charge carriers, the electrons, the O^+ ion, and the O^- ion. Furthermore, there are several minority species like O_2^+, O_2^-, and O_3^-, which can be ignored in the energy flux balance.[21] Negative ions also cannot reach the substrate, unless $V_S \gg 0$, and even in that case their energy is limited. Therefore, they can be ignored in the flux equations. Nevertheless, the presence of negative ions does alter the discharge. In most cases, the negative ion density will exceed the electron density thus $n_e \ll n_+$. Moreover, the transport properties and sheath structure are different in an electronegative plasma.[32] Thus, appropriate changes have to be made to Eqs. (5)–(9).[15] This also makes the interpretation of the probe measurements of the plasma parameters more complicated.

Nevertheless, treatment of the charged species energy flux is relatively straightforward. An accurate estimate of the neutral species contribution to the energy flux is more complex because of the molecular nature of oxygen. Like argon,

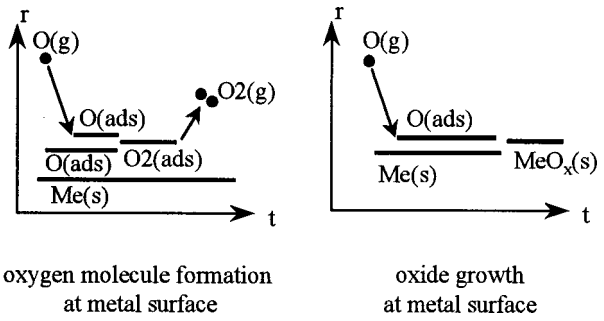

FIG. 11. Reaction graph for oxygen molecule formation (association) and substrate oxidation.

oxygen can be electronically excited. In addition, the oxygen molecules in general will have rovibrational energy. Association reactions of oxygen atoms forming oxygen molecules have also to be taken into account. However, the reaction probabilities for rovibrational deexcitation and association on a surface exposed to a discharge are poorly known. Nor is the final state of the reaction products known. In a previous study, these reactions were shown to have a major impact on the plasma characteristics.[21] Under our conditions, oxidation of the copper probe surface is expected only in the initial stage of probe usage, resulting in the formation of a passivating layer. Thus, this term can be neglected, but in general, reactions with the probe surface have also to be considered. The principles of both mechanisms are illustrated by schematic reaction graphs in Fig. 11.

As a complete treatment of an oxygen discharge is beyond the scope of this article, in Fig. 12, we only compare thermal probe measurements of the energy influx to the substrate in an O_2 and an argon plasma under the same macroscopic conditions (1 Pa, 15 W, same geometry). It is obvious that the total energy influx for oxygen is higher than for argon. The decreased slope for $V_S<0$ with respect to argon indicates that in contrast to argon, in the oxygen plasma the main contribution to the energy flux is caused by neutral species.

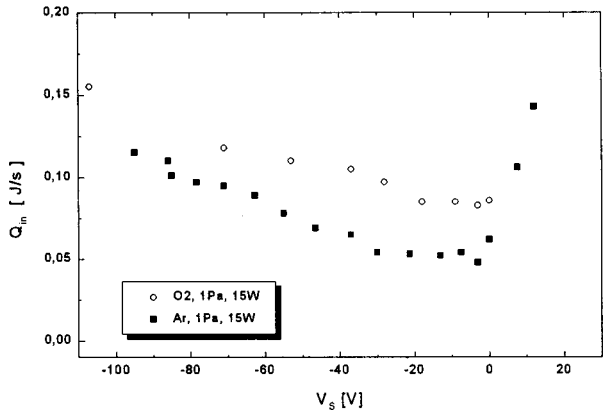

FIG. 12. Measured integral energy influx (Q_{in}) for argon and oxygen, respectively, for the same macroscopic discharge conditions.

V. CONCLUSION

The total energy influx ($J_{in}=Q_{in}/A_S$) from a low power argon rf plasma (1 Pa, 15 W) towards a metal substrate has been determined by a thermal probe to be in the order of $6\times10^{-3}-3\times10^{-3}$ J/cm^2 s for negative substrate voltages in the range of $-100-0$ V where the ions are the dominant species for surface heating. For positive V_S, the flux is in the order of $3\times10^{-3}-8\times10^{-3}$ J/cm^2 s and the kinetic energy of the electrons is the main source for surface heating. The complete kinetic energy of the charge carriers is transferred into substrate heating. In case of an oxygen rf plasma under the same experimental conditions, the energy influx J_{in} for $V_S=-110-0$ V is in the order of $9\times10^{-3}-5\times10^{-3}$ J/cm^2 s which is about 50% higher than for argon at the same substrate voltages. In contrast to argon, in oxygen, the main contribution to the energy influx is by neutral species and not by charge carriers. In both cases, the deposited thermal power is rather low in comparison to other plasma processes as sputtering or surface cleaning,[18] but probably comparable to the thermal load of macroscopic particles suspended in the discharge.[11] The results underline the sensitivity of the thermal probe method and its capability to separate several contributions to the total thermal influx.

ACKNOWLEDGMENTS

The work has been supported by the Deutsche Forschungsgemeinschaft (DFG) under SFB198/A14. The authors wish to express their thanks to A. Knuth. E.S., and W.W.S. wish to acknowledge the support of the Royal Dutch Academy of Science (KNAW).

[1] J. A. Thornton, J. Vac. Sci. Technol. **11**, 666 (1974).
[2] H. Deutsch, H. Kersten, and A. Rutscher, Contrib. Plasma Phys. **29**, 263 (1989).
[3] H. Deutsch, H. Kersten, S. Klagge, and A. Rutscher, Contrib. Plasma Phys. **28**, 149 (1988).
[4] S. D. Bernstein, T. Y. Wong, and R. W. Tustison, J. Vac. Sci. Technol. B **12**, 605 (1994).
[5] H. Brune, H. Roder, K. Bromann, and K. Kern, Thin Solid Films **264**, 230 (1995).
[6] H. Windischmann, J. Appl. Phys. **62**, 1800 (1987).
[7] K. H. Müller, Appl. Phys. **40**, 209 (1986).
[8] R. Piejak, V. Godyak, B. Alexandrovich, and N. Tishchenko, Plasma Source Sci. Technol. **7**, 590 (1998).
[9] M. Andritschky, F. Guimaraes, and V. Teixeira, Vacuum **44**, 809 (1993).
[10] H. Kersten, G. M. W. Kroesen, and R. Hippler, Thin Solid Films **332**, 282 (1998).
[11] G. H. P. M. Swinkels, Proceedings of Dusty Plasma Conference, Col de Porte, France, January, 1999.
[12] B. Hussla, K. Enke, H. Grünwald, G. Lorenz, and H. Stoll, J. Phys. D: Appl. Phys. **20**, 889 (1987).
[13] H. Kersten, H. Steffen, D. Vender, and H. E. Wagner, Vacuum **46**, 305 (1995).
[14] D. Bohm, in *The Characteristics of Electrical Discharges in Magnetic Fields*, edited by A. Guthrie and R. K. Wakerling (McGraw-Hill, New York, 1949).
[15] E. Stoffels, W. W. Stoffels, D. Vender, M. Haverlag, G. M. W. Kroesen, and F. J. deHoog, Contrib. Plasma Phys. **35**, 331 (1995).
[16] *CRC Handbook of Chemistry and Physics*, 75th ed., edited by P. R. Lide and H. P. Frederikse (CRC, Boca Raton, FL, 1994).
[17] H. Kersten, R. J. M. M. Snijkers, J. Schulze, G. M. W. Kroesen, H. Deutsch, and F. J. deHoog, Appl. Phys. Lett. **64**, 1496 (1994).
[18] H. Kersten, H. Deutsch, and J. F. Behnke, Vacuum **48**, 123 (1997).
[19] E. Meeks, P. Ho, A. Ting, and R. J. Buss, J. Vac. Sci. Technol. A **16**, 2227 (1998).

[20] E. Stoffels and W. W. Stoffels, Ph.D. thesis, Eindhoven University of Technology, Eindhoven, The Netherlands, 1994.
[21] E. Stoffels, W. W. Stoffels, D. Vender, M. Kando, G. M. W. Kroesen, and F. J. deHoog, Phys. Rev. E **51**, 2425 (1995).
[22] H. Kersten, D. Rohde, J. Berndt, H. Deutsch, and R. Hippler, Thin Solid Films (submitted).
[23] J. A. Thornton, Thin Solid Films **54**, 23 (1978).
[24] R. Wendt, K. Ellmer, and K. Wiesemann, J. Appl. Phys. **82**, 2115 (1997).
[25] H. Steffen, H. Kersten, and H. Wulff, J. Vac. Sci. Technol. A **12**, 2780 (1994).
[26] V. A. Godyak, R. B. Piejak, and B. R. Alexandrovich, Plasma Source Sci. Technol. **1**, 36 (1992).
[27] S. Pfau, J. Rohmann, D. Uhrlandt, and R. Winkler, Contrib. Plasma Phys. **36**, 449 (1996).
[28] R. Seeliger, *Einführung in die Physik der Gasentladungen* (J. A. Barth, Leipzig, 1926).
[29] M. Schmidt, F. Hempel, M. Hannemann, and R. Foest, Bull. Am. Phys. Soc. **42**, 1733 (1997).
[30] W. Goedheer, Proceedings of Dusty Plasma Conference, Noordwijkerhout, The Netherlands, January 1998.
[31] H. Toyoda and H. Sugai, J. Plasma Fusion Res. **75**, 779 (1999).
[32] D. Vender, W. W. Stoffels, E. Stoffels, G. M. W. Kroesen, and F. J. deHoog, Phys. Rev. E **51**, 2436 (1995).